Spatiotemporal Concentration Patterns in a Surface Reaction: Propagating and Standing Waves, Rotating Spirals, and Turbulence

S. Jakubith, H. H. Rotermund, W. Engel, A. von Oertzen, and G. Ertl

Fritz-Haber-Institut der Max-Planck-Gesellschaft, Faradayweg 4-6, D-1000 Berlin 33, Germany

(Received 25 June 1990)

Laterally varying surface concentrations associated with the oscillatory oxidation of carbon monoxide on a Pt(110) surface were imaged by photoemission electron microscopy. Depending on the applied conditions, a large variety of spatiotemporal patterns were observed that are characteristic for the nonlinear dynamics of reaction-diffusion systems.

PACS numbers: 68.35.−p, 82.65.−i

Chemical reactions far from equilibrium may exhibit, even if operated under stationary continuous-flow conditions, various phenomena of temporal and spatial self-organization. Effects belonging in these categories have already been widely investigated, both experimentally and theoretically, with homogeneous reactions in solution, in particular, with the famous Belousov-Zhabotinskii (BZ) reaction.[1] Corresponding studies with heterogeneous reactions occurring at well-defined single-crystal surfaces were initiated only more recently.[2] Among the latter, the catalytic oxidation of CO on a Pt(110) surface was found to exhibit a very rich variety of oscillatory kinetics. The underlying microscopic mechanism has been explored in great detail, enabling satisfactory theoretical modeling of the temporal behavior.[2,3] Generally, the occurrence of temporal variations of the concentrations of the species involved in the reaction implies that these also vary spatially, unless local differences are eliminated by "stirring," i.e., rapid convection. With the BZ reaction (and other homogeneous reactions in solution), the resulting spatiotemporal concentration patterns can easily be made visible by the associated color differences. More refined techniques are, however, required to image local variations of surface properties. For example, recent attempts to image patterns associated with the CO oxidation reaction include the application of scanning low-energy electron diffraction,[4] as well as scanning photoemission microscopy[5] (SPM) and photoemission electron microscopy (PEEM).[6] The latter technique is particularly versatile due to its high temporal (~ 10 ms) and lateral (~ 0.1 μm) resolution, and a newly designed instrument of this type[7] was applied in the present work to image an unprecedented rich variety of spatiotemporal patterns associated with the oscillatory reaction of catalytic CO oxidation on Pt(110).

The principle of the PEEM technique consists in illuminating the sample surface with UV light from a deuterium lamp (with its cutoff near 6.9-eV photon energy) and to image the lateral intensity distribution of the photoemitted electrons through a system of electrostatic lenses after amplification by a channel plate onto a "back-view" fluorescence screen. The intensity of photoemitted electrons depends on the (local) work function

Φ which in turn is affected by the dipole moments of the adsorbate complexes.

In the current investigation, Φ of a clean Pt(110) surface increases 0.3 eV when saturated with CO, and 0.5 eV through oxygen chemisorption. Therefore, areas covered by O_{ad} appear dark in the images, while those covered by CO_{ad} are brighter. A sample with dimensions of about 6×10 mm^2 was mounted on a manipulator capable of well-defined displacements through a set of stepping motors. By looking at different locations it was ascertained that the images were representative for the whole macroscopic surface area. The total photocurrent is in the nA range and can be measured independently. It reflects the spatially integrated behavior of the system.

The PEEM instrument is attached to a UHV system containing standard facilities for cleaning and characterizing sample surfaces. The temporal behavior of the present system has been studied previously in detail.[8,9] Depending on the control parameters, temperature T as well as CO and O$_2$ partial pressures p_{CO} and p_{O_2}, a rich variety of kinetic effects have been observed, ranging from regular to irregular, relaxation-type oscillations to chaos. In the current study, the scenario of associated *spatial* patterns turned out to be even richer. We present data for a few typical cases at two ranges of temperature demonstrating two types of characteristic behavior. The experiments were performed with p_{O_2} and T fixed at preset values; then p_{CO} was varied in small increments until the onset of self-organization was observed. Subsequently, all the control parameters were held strictly constant while the images were taken.

Figure 1 shows a series of PEEM images consequently recorded at $T = 427$ K, $p_{CO} = 3.0 \times 10^{-5}$ mbar, and $p_{O_2} = 3.2 \times 10^{-4}$ mbar. The images exhibit concentric, elliptically shaped waves emanating periodically from nucleation centers ("pacemakers") and propagating with anisotropic velocities. Higher propagation velocities along the longer axis of these ellipses (4.2 μm/sec) coincide with the [1$\bar{1}$0] orientation of the Pt(110) single-crystal surface, while the shorter axis (velocity about 1.5 μm/sec) parallels the [001] orientation of the substrate lattice. This effect presumably reflects the anisotropy of the surface diffusion coefficients of the adsorbates which are expected to be highest along the troughs formed by
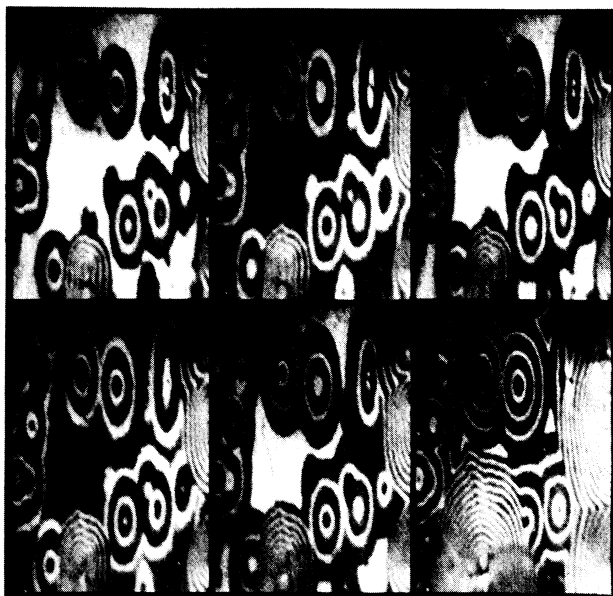
FIG. 1. Sequence of target patterns on a 0.2×0.3-mm^2 section of the Pt(110) surface at $T=427$ K, $p_{CO}=3\times10^{-5}$ mbar, and $p_{O_2}=3.2\times10^{-4}$ mbar. The time interval between the first five images is 4.1 sec; the time interval between the last two images is 30 sec.

FIG. 2. Growth of a spiral wave. Width of each image 0.2 mm. $T=434$ K, $p_{CO}=2.8\times10^{-5}$ mbar, and $p_{O_2}=3.0\times10^{-4}$ mbar. $t=0$, 10, 21, 39, 56, and 74 sec.

the densely packed atomic rows along the [1$\bar{1}$0] direction and which affect the propagation velocity of a "chemical" wave caused by reaction-diffusion coupling.[10] The pacemakers oscillate with a frequency of about 0.15 sec^{-1}, thus giving rise to wavelengths of the order of 30 and 10 μm in the [1$\bar{1}$0] and [001] directions, respectively. Theoretical analysis of the BZ reaction revealed that the speed of propagation is affected by the curvature of the wave front,[11] as also verified experimentally,[12] an effect which will have to be explored with the present system in future work.

Expanding target patterns observed for the BZ reaction[13] feature properties quite similar to those in the present case. For example, upon collision of two elliptic waves these annihilate each other and consequently lead to the formation of cusplike structures, as can be seen in the lower series of images in Fig. 1. In addition to the elliptic waves, Fig. 1 shows features with considerably shorter wavelengths growing in from the lower and right-hand margins. These develop as expanding spirals rather than from closed wave fronts and will be discussed in more detail in connection with Fig. 2.

In Fig. 1, in addition to the patterns on the <0.1-mm length scale, the whole background varies in intensity as evident from the first five images in this series where the regions between the concentric waves switch periodically from bright (CO covered) to dark (O covered). This effect parallels the associated relaxation-type oscillations of the (integral) reaction rate. The switching of the background intensity occurs within about 1 sec over the entire surface area. This indicates the operation of gas-phase coupling as an additional (i.e., apart from reaction-diffusion coupling) and rapid synchronization mechanism for this system, as discussed elsewhere.[14]

As a whole, each pacemaker oscillates at a higher frequency than the rest and periodically emanates reaction-diffusion waves, in qualitative agreement with relevant theories.[15] Each time the medium undergoes a bulk transition, the outermost wave is annihilated, but the target pattern as a whole grows slowly since subsequent waves propagate beyond the zone of last annihilation, as is nicely demonstrated in Fig. 1. Although the nature of the pacemakers is still quite unclear (similar to the BZ reaction), it is quite likely that these are formed by a certain type of surface imperfection, which is supported by the observation that the target patterns will usually reappear at the same spots if the experiment is repeated.

Figure 2 reproduces a series of images which were taken under slightly different conditions, showing the continuous growth of a spiral wave. Again, the ellipticity of the spirals is attributed to the anisotropy of the surface diffusion coefficient. The wave fronts propagate at 3.3 and 1.2 μm/sec into the two directions, respectively. In contrast to the case shown in Fig. 1, the system does not exhibit self-sustained temporal oscillations but behaves as an excitable medium. Analogous observations with the BZ reaction were first made by Winfree[16] who also provided a simple qualitative interpretation for the origin of the spirals on the basis of numerical simulation.[17]

Following the general mathematical proof of the existence of rotating spiral solutions of reaction-diffusion equations,[18] this problem was treated in several papers, either by solving the underlying partial differential equations[11] or by computer simulation.[19] For the formation of spirals no heterogeneity at the center is needed, only a certain topological condition must be satisfied by the initial concentration distribution,[1(b)] as offered, most simply, by the broken end of a wave front.

The second set of data to be presented was recorded at higher temperature (550 K) in the range of p_{CO} and p_{O_2} conditions within which the system may, inter alia, exhibit regular harmonic temporal oscillations at periods of only a few seconds.[8,9] Previous experiments with lateral resolution > 1 mm had indicated that, under these conditions, the macroscopic properties of the surface changed in phase and propagating-wave phenomena were not observed. This supported the concept that gas-phase coupling is the dominant synchronization mechanism, suggesting that concentrations depend only on time but not on space. It remained unclear, however, down to which length uniform spatial coverage would persist. It turned out that these oscillations are indeed associated with breaking of the local symmetry on a scale of around 10 μm.

The series of images in Fig. 3 illustrates the type of patterns associated with the quoted regular oscillations and their variations during about one-third of the length of the period. There are no longer propagating waves;

rather, standing waves were observed, reflecting rapidly varying surface concentrations of the reacting species with additional spatial modulations. The relaxation time for synchronization between different regions is shorter than 10^{-2} sec, the current temporal resolution with our technique. Gas-phase coupling occurs with a time constant of about 10^{-4} sec, as determined by the molecular speed of the gaseous reactants and the dimensions of the UHV vessel.

We do not yet know what determines the positions of and spacings between the standing waves seen in Fig. 3. Interestingly, these spacings are not precisely constant but may vary even between neighboring pairs. This causes the formation of dynamic "dislocations," as evident from Fig. 3.

As time goes by, these dislocation lines may increase in density, and may even exhibit varying orientations so that they eventually intersect each other. A result of this type is shown in Fig. 4 where the separation between two dislocation lines equals about half of the wavelength of the standing wave, giving rise to rhomb-shaped spatiotemporal patterns.

If one of the control parameters is varied (say, decrease of p_{CO}) in rather small steps, the temporal behavior undergoes a transition from regular oscillations to chaos via a sequence of period doublings.[8,9] The associated patterns become increasingly irregular, but spatial patterns are still observed even outside the range of oscillations, i.e., when the temporal behavior is stationary.
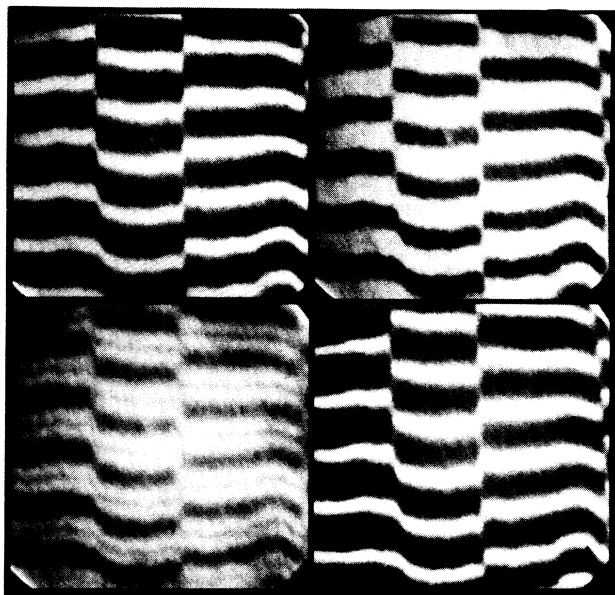

FIG. 3. Standing-wave-type patterns on a 0.3×0.3-mm^2 surface area accompanying rapid harmonic temporal oscillations with a period duration of $\tau = 1.4$ sec. $T = 550$ K, $p_{CO} = 1.75 \times 10^{-4}$ mbar, and $p_{O_2} = 4.1 \times 10^{-4}$ mbar. $t = 0$, 0.08, 0.12, and 0.46 sec.
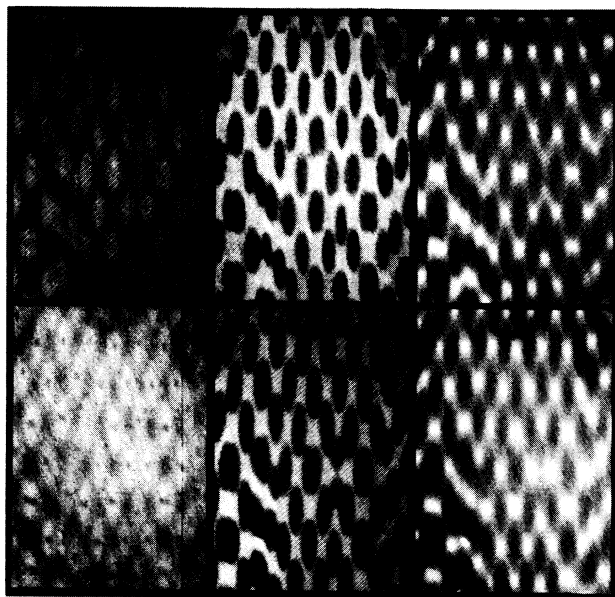

FIG. 4. Standing-wave patterns on a 0.2×0.3-mm^2 surface area associated with regular temporal oscillations with a period duration of $\tau = 2.8$ sec. $T = 544$ K, $p_{CO} = 1.2 \times 10^{-4}$ mbar, and $p_{O_2} = 3.1 \times 10^{-4}$ mbar. $t = 0$, 0.6, 0.8, 1.4, 2.0, and 2.2 sec.
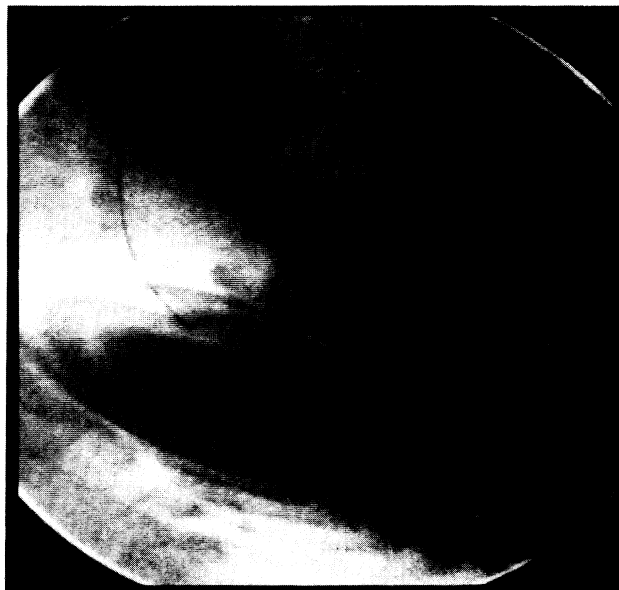
FIG. 5. Pattern from a 0.35×0.35-mm^2 surface area exhibiting chemical turbulence. $T = 544$ K, $p_{CO} = 1.0 \times 10^{-4}$ mbar, and $p_{O_2} = 3.1 \times 10^{-4}$ mbar.

For conditions prior to the onset of oscillations, i.e., for p_{CO} slightly larger than that for the Hopf bifurcation, irregular stripes are observed which now, however, propagate fairly rapidly across the surface, rather than forming standing waves. Beyond the sequence of period doublings, on the other hand, patterns of the kind shown in Fig. 5 appear. They consist of rapidly moving irregular wave fronts, rotating spirals, etc., and are strongly reminiscent of the flow patterns of hydrodynamic turbulence.

In conclusion, the present work demonstrates the occurrence of a rich scenario of spatiotemporal patterns accompanying the oscillatory CO oxidation reaction on a Pt(110) surface. Theoretical modeling will have to start from the known reaction mechanism by extending the ordinary differential equations describing the (spatially averaged) temporal behavior.[3]

[1]See, e.g., (a) *Oscillations and Traveling Waves in Chemical Systems,* edited by R. J. Field and M. Burger (Wiley, New York, 1985); (b) Y. Kuramoto, *Chemical Oscillations, Waves and Turbulence* (Springer-Verlag, Berlin, 1984).

[2]R. Imbihl, in *Optimal Structures in Heterogeneous Reaction Systems,* edited by P. J. Plath (Springer-Verlag, Berlin, 1989), p. 26; G. Ertl, Adv. Catal. (to be published).

[3]R. M. Eiswirth, K. Krischer, and G. Ertl, Appl. Phys. A **51**, 79 (1990).

[4]M. P. Cox, G. Ertl, and R. Imbihl, Phys. Rev. Lett. **54**, 1725 (1985).

[5]H. H. Rotermund, S. Jakubith, A. von Oertzen, and G. Ertl, J. Chem. Phys. **91**, 4942 (1989).

[6]M. E. Kordesch, W. Engel, G. Lapeyre, E. Zeitler, and A. M. Bradshaw, Appl. Phys. Lett. A **49**, 399 (1989); M. Mundschau, M. E. Kordesch, B. Rausenberger, W. Engel, A. M. Bradshaw, and E. Zeitler, Surf. Sci. **227**, 246 (1990); H. H. Rotermund, W. Engel, M. E. Kordesch, and G. Ertl, Nature (London) **343**, 355 (1990).

[7]W. Engel, H. H. Rotermund, M. Kordesch, S. Kubala, A. v. Oertzen, and S. Jakubith, in Proceedings of the Twelfth International Congress for Electron Microscopy, Seattle, WA, 1990 (to be published).

[8]M. Eiswirth and G. Ertl, Surf. Sci. **177**, 90 (1986).

[9]M. Eiswirth, K. Krischer, and G. Ertl, Surf. Sci. **202**, 565 (1988).

[10]J. Ross, S. C. Müller, and C. Vidal, Science **240**, 460 (1988); J. J. Tyson, in Ref. 1(a), p. 93; R. Arnold, K. Showalter, and J. Tyson, J. Chem. Educ. **64**, 740 (1987).

[11]J. J. Tyson and J. P. Keener, Physica (Amsterdam) **21D**, 307 (1986); **32D**, 327 (1988).

[12]P. Foerster, S. C. Müller, and B. Hess, Science **241**, 685 (1988).

[13]A. N. Zaikin and A. M. Zhabotinski, Nature (London) **225**, 535 (1970).

[14]M. Eiswirth, P. Möller, K. Wetzl, R. Imbihl, and G. Ertl, J. Chem. Phys. **90**, 510 (1989).

[15]P. Ortoleva and J. Ross, J. Chem. Phys. **58**, 5673 (1973); J. J. Tyson and P. C. Fife, J. Chem. Phys. **73**, 2224 (1980).

[16]A. T. Winfree, Science **175**, 634 (1972).

[17]A. T. Winfree, Sci. Am. **230**, 82 (1974).

[18]A. S. Mikhailov and V. I. Krinski, Physica (Amsterdam) **9D**, 346 (1983).

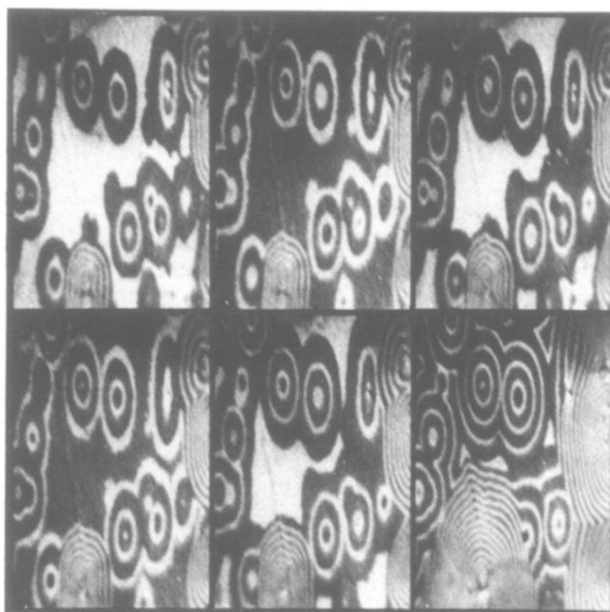[19]M. Gerhardt and H. Schuster, Physica (Amsterdam) **36D**, 209 (1989).

FIG. 1. Sequence of target patterns on a 0.2×0.3-mm^2 section of the Pt(110) surface at $T = 427$ K, $p_{CO} = 3 \times 10^{-5}$ mbar, and $p_{O_2} = 3.2 \times 10^{-4}$ mbar. The time interval between the first five images is 4.1 sec; the time interval between the last two images is 30 sec.
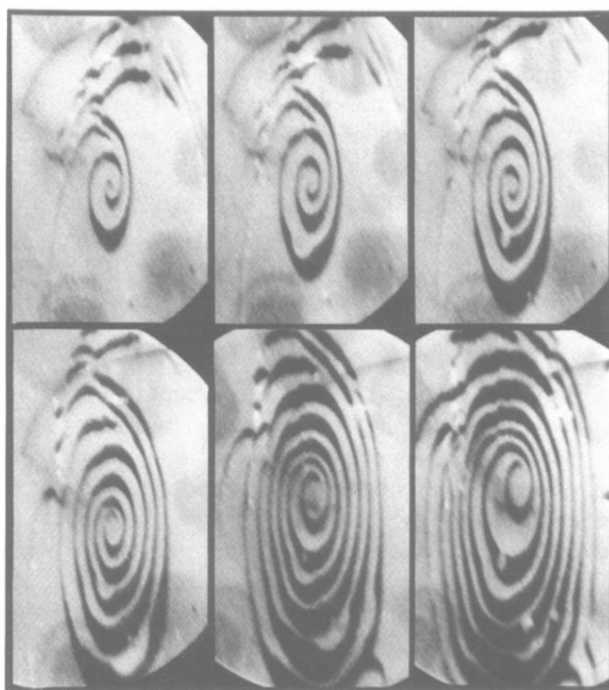
FIG. 2. Growth of a spiral wave. Width of each image 0.2 mm. $T = 434$ K, $p_{CO} = 2.8 \times 10^{-5}$ mbar, and $p_{O_2} = 3.0 \times 10^{-4}$ mbar. $t = 0, 10, 21, 39, 56,$ and 74 sec.
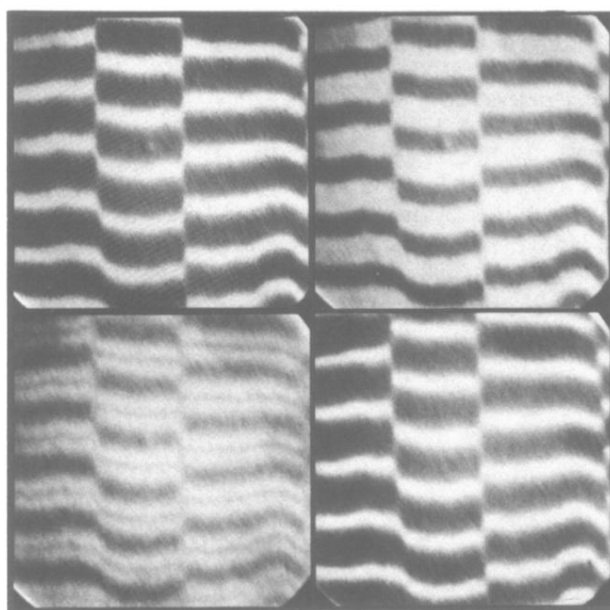
FIG. 3. Standing-wave-type patterns on a 0.3×0.3-mm^2 surface area accompanying rapid harmonic temporal oscillations with a period duration of $\tau = 1.4$ sec. $T = 550$ K, $p_{CO} = 1.75 \times 10^{-4}$ mbar, and $p_{O_2} = 4.1 \times 10^{-4}$ mbar. $t = 0$, 0.08, 0.12, and 0.46 sec.
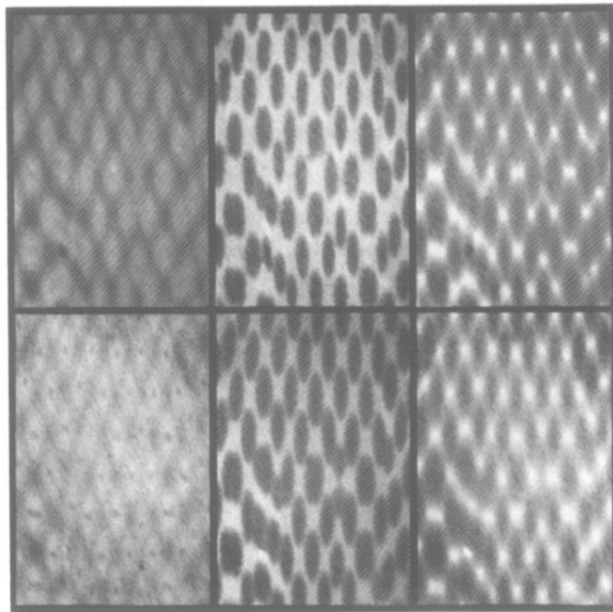
FIG. 4. Standing-wave patterns on a 0.2×0.3-mm^2 surface area associated with regular temporal oscillations with a period duration of $\tau = 2.8$ sec. $T = 544$ K, $p_{CO} = 1.2 \times 10^{-4}$ mbar, and $p_{O_2} = 3.1 \times 10^{-4}$ mbar. $t = 0$, 0.6, 0.8, 1.4, 2.0, and 2.2 sec.
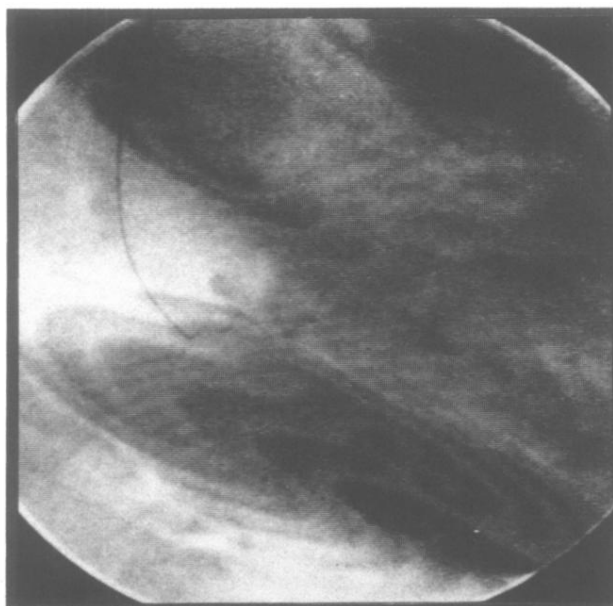
FIG. 5. Pattern from a 0.35×0.35-mm^2 surface area exhibiting chemical turbulence. $T = 544$ K, $p_{CO} = 1.0 \times 10^{-4}$ mbar, and $p_{O_2} = 3.1 \times 10^{-4}$ mbar.